

Hadronic form factors and the J/ψ secondary production cross section: an update

¹F. Carvalho, ²F.O. Durães, ³F.S. Navarra and ³M. Nielsen

¹*Instituto de Física Teórica, Universidade Estadual Paulista
Rua Pamplona, 145, 01405-000, São Paulo - S.P.*

²*Universidade Presbiteriana Mackenzie, C.P. 01302-907 São Paulo, Brazil* ³*Instituto de Física, Universidade de São Paulo
C.P. 66318, 05315-970 São Paulo, SP, Brazil*

Improving previous calculations, we compute the $D + \bar{D} \rightarrow J/\psi + \pi$ cross section using the most complete effective lagrangians available. The new crucial ingredients are the form factors on the charm meson vertices, which are determined from QCD sum rules calculations. Some of them became available only very recently and the last one, needed for our present purpose, is calculated in this work.

I. INTRODUCTION

Before RHIC, RHIC physics was relatively simple. We were basically searching for a quasi-ideal gas of deconfined quarks and gluons (QGP). One of the best signatures of this new state of matter was charmonium suppression [1]. During the last four years, due to intense work both theoretical and experimental, this naive picture changed drastically. On the theoretical side, careful numerical simulations [2–5] have shown that, due to the importance of charm recombination in the deconfined phase and also to final state interactions, the number of J/ψ 's may stay approximately the same. From the experimental side, especially from the analysis of elliptic flow, came the conclusion that the new state of matter is not a gas, being rather a strongly interacting fluid, now called sQGP [6]. Taking the existing calculations seriously, it is no longer clear that an overall suppression of the number of J/ψ 's will be a signature of QGP. A more complex pattern can emerge, with suppression in some regions of the phase space and enhancement in others [7,8]. Whatever the new QGP signature (involving charm) turns out to be, it is necessary to understand better the mechanisms of J/ψ production and dissociation by collisions with comoving hadrons.

A great effort has been dedicated to understand J/ψ dissociation in a hadronic environment. Since there is no direct experimental information on J/ψ absorption cross sections by hadrons, several theoretical approaches have been proposed to estimate their values. One approach was based on charm quark-antiquark dipoles interacting with the gluons of a larger (hadron target) dipole. This is the Bhanot-Peskin (BP) approach [9], which was rediscovered by Kharzeev and Satz [10] in the mid-nineties and updated [11,12] in the last years. Finally, the recent next to leading order calculations presented in [13] have conclusively shown that, for charmonium, the formalism breaks down because this system is not heavy enough. Also considered was quark exchange between two (hadronic) bags [14,15]. The most explored approach has been the meson exchange mechanism [16–20]. In our opinion the most reliable calculations of $\sigma_{J/\psi-\pi}$ was done with QCD sum rules [21]. However, due to a low momentum approximation, the validity of this calculation was restricted to low energy reactions, close to the dissociation threshold. This is probably not enough for the numerical simulations mentioned above. Therefore, in order to have cross sections valid at higher energies, the effective lagrangian approach still remains the most appropriate option.

After many works on the subject some consensus has been achieved, at least in what concerns the determination of the order of magnitude, which, in the case of the J/ψ pion interaction, is determined to be $1 < \sigma_{J/\psi-\pi} < 10$ mb in the energy region close to the open charm production threshold.

Once the J/ψ dissociation cross section is known, using detailed balance one can attempt to estimate the charmonium formation cross section through the fusion of open charm, as, for example, $D\bar{D} \rightarrow J/\psi + \pi$. This is known as secondary charmonium production. As it was first pointed out in [22], in nucleus - nucleus collisions at sufficiently high energies, the number of produced D and D^* mesons increases and also the lifetime of the hadronic fireball increases. It becomes then possible that a significant number of J/ψ 's be formed by open charm fusion. Later, an estimate made in [23] indicated that this mechanism would be relevant only for LHC energies. The authors stressed, however, that their conclusion was very sensitive to the value of the J/ψ formation cross section, or equivalently to the absorption cross section, which in that case was the one computed with the Bhanot-Peskin approach. The subject was left aside for some time. Recently, after the revision of the J/ψ absorption cross section to larger values,

secondary J/ψ production was incorporated in event generators in [24] and [5]. According to these simulations, the number of secondary J/ψ 's is significant already at RHIC energies.

Given the renewed interest on the subject we shall, in this work, further refine our estimate of the J/ψ interaction cross section, giving now emphasis to secondary charmonium production. We shall employ effective lagrangians with form factors calculated with QCDSR. In particular, in the present calculation we shall make use of the D^*D^*J/ψ form factor, which was obtained only very recently [25] and we shall also calculate the $D^*D^*\pi$ form factor, which had not been calculated so far.

II. THE EFFECTIVE LAGRANGIANS

Since the pioneering work of Muller and Matynian [16], there has been an intense discussion concerning the details and properties of the effective lagrangians which describe the interactions among charm mesons. Here we do not add anything new to this discussion. We shall use what we believe is the state - of - the - art lagrangian. For the sake of completeness and for future use we present below the effective lagrangians considered in this work:

$$\mathcal{L}_{D^*D\pi} = ig_{D^*D\pi}(D_\mu^*\partial^\mu\pi\bar{D} - D\partial^\mu\pi\bar{D}_\mu^*) \quad (1)$$

$$\mathcal{L}_{\psi D^*D} = g_{\psi D^*D}\epsilon^{\mu\nu\alpha\beta}\partial_\mu\psi_\nu(\partial_\alpha D_\beta^*\bar{D} + D\partial_\alpha\bar{D}_\beta^*) \quad (2)$$

$$\mathcal{L}_{\psi DD\pi} = ig_{\psi DD\pi}\epsilon^{\mu\nu\alpha\beta}\psi_\mu\partial_\nu D\partial_\alpha\pi\bar{D}_\beta \quad (3)$$

$$\mathcal{L}_{\psi DD} = -ig_{\psi DD}\psi^\mu(\partial_\mu D\bar{D} - D\partial_\mu\bar{D}) \quad (4)$$

$$\mathcal{L}_{D^*D^*\pi} = -g_{D^*D^*\pi}\epsilon^{\mu\nu\alpha\beta}\partial_\mu D_\nu^*\pi\partial_\alpha\bar{D}_\beta^* \quad (5)$$

$$\begin{aligned} \mathcal{L}_{\psi D^*D^*} = & ig_{\psi D^*D^*}[\psi^\mu(\partial_\mu D^{*\nu}\bar{D}_\nu^* - D^{*\nu}\partial_\mu\bar{D}_\nu^*) \\ & + (\partial_\mu\psi_\nu D^{*\nu} - \psi_\nu\partial_\mu D_\nu^*)D^{*\mu} + D^{*\mu}(\psi^\nu\partial_\mu\bar{D}_\nu^* - \partial_\mu\psi_\nu\bar{D}^{*\nu})] \end{aligned} \quad (6)$$

$$\mathcal{L}_{\psi D^*D\pi} = -g_{\psi D^*D\pi}\psi^\mu(D\pi\bar{D}_\mu^* + D_\mu^*\pi\bar{D}) \quad (7)$$

$$\mathcal{L}_{\psi D^*D^*\pi} = ig_{\psi D^*D^*\pi}\epsilon^{\mu\nu\alpha\beta}\psi_\mu D_\nu^*\partial_\alpha\pi\bar{D}_\beta^* + ih_{\psi D^*D^*\pi}\epsilon^{\mu\nu\alpha\beta}\partial_\mu\psi_\nu D_\alpha^*\pi\bar{D}_\beta^* \quad (8)$$

With these lagrangians we are able to compute the processes $D\bar{D} \rightarrow J/\psi + \pi$, which involves the diagrams in Figure 1, the process $D^*\bar{D} \rightarrow J/\psi + \pi$, corresponding to the diagrams shown in Figure 2 and also the process $D^*\bar{D}^* \rightarrow J/\psi + \pi$, corresponding to the diagrams in Figure 3.

Calling p_1 and p_2 the four-momenta of the incoming particles and p_3 and p_4 the four-momenta of the outgoing particles, we can derive the Feynman rules from the above lagrangians and obtain the invariant amplitudes for each one of the processes in Figures 1, 2 and 3. They are given by:

$$\mathcal{M}_\mu^{1a} = -g_{D^*D\pi}p_{3\alpha}\frac{1}{t-m_{D^*}^2}\left(g_{\alpha\beta}-\frac{q_\alpha q_\beta}{m_{D^*}^2}\right)g_{\psi D^*D}\epsilon^{\rho\mu\theta\beta}q_\theta p_{4\rho} \quad (9)$$

$$\begin{aligned} \mathcal{M}_\mu^{1b} = & g_{D^*D\pi}p_{3\alpha}\frac{1}{u-m_{D^*}^2}\left(g_{\alpha\beta}-\frac{(p_2-p_3)_\alpha(p_2-p_3)_\beta}{m_{D^*}^2}\right) \times \\ & g_{\psi D^*D}\epsilon^{\rho\mu\theta\beta}(p_2-p_3)_\theta p_{4\rho} \end{aligned} \quad (10)$$

$$\mathcal{M}_\mu^{1c} = g_{\psi D^*D\pi}\epsilon^{\mu\rho\theta\delta}p_{1\rho}p_{2\delta}p_{3\theta} \quad (11)$$

$$\mathcal{M}_{\nu\sigma}^{2a} = g_{D^*D\pi}p_{3\nu}\frac{1}{t-m_D^2}g_{\psi DD}(p_2-q)_\sigma \quad (12)$$

$$\mathcal{M}_{\nu\sigma}^{2b} = g_{\pi D^*D^*}\epsilon^{\gamma\nu\delta\alpha}p_{1\gamma}q_\delta\frac{1}{t-m_{D^*}^2}\left(g_{\alpha\beta}-\frac{q_\alpha q_\beta}{m_{D^*}^2}\right)g_{\psi D^*D}\epsilon^{\rho\sigma\theta\beta}p_{4\rho}q_\theta \quad (13)$$

$$\mathcal{M}_{\nu\sigma}^{2c} = g_{D^*D\pi} p_{3\alpha} \frac{1}{u - m_{D^*}^2} \left(g_{\alpha\beta} - \frac{(p_2 - p_3)_\alpha (p_2 - p_3)_\beta}{m_{D^*}} \right) \times \\ g_{\psi D^* D^*} \left[(p_1 - p_2 + p_3)_\sigma g_{\nu\beta} - (p_1 + p_4)_\beta g_{\nu\sigma} + (p_2 - p_3 + p_4)_\nu g_{\sigma\beta} \right] \quad (14)$$

$$\mathcal{M}_{\nu\sigma}^{2d} = -g_{\psi D^* D\pi} g_{\nu\sigma} \quad (15)$$

$$\mathcal{M}_{\mu\nu\sigma}^{3a} = g_{D^*D\pi} p_{3\mu} \frac{1}{t - m_D^2} g_{\psi D^* D} \epsilon^{\rho\sigma\theta\nu} p_{4\rho} p_{2\theta} \quad (16)$$

$$\mathcal{M}_{\mu\nu\sigma}^{3b} = -g_{D^*D\pi} p_{3\nu} \frac{1}{u - m_D^2} g_{\psi D^* D} \epsilon^{\rho\sigma\theta\mu} p_{4\rho} p_{1\theta} \quad (17)$$

$$\mathcal{M}_{\mu\nu\sigma}^{3c} = g_{\pi D^* D^*} \epsilon^{\delta\mu\theta\alpha} p_{1\delta} q_\theta \frac{1}{t - m_{D^*}^2} \left(g_{\alpha\beta} - \frac{q_\alpha q_\beta}{m_{D^*}} \right) \times \\ g_{\psi D^* D^*} \left[(q - p_2)_\sigma g_{\nu\beta} + (p_2 + p_4)_\beta g_{\nu\sigma} - (p_4 + q)_\nu g_{\sigma\beta} \right] \quad (18)$$

$$\mathcal{M}_{\mu\nu\sigma}^{3d} = -g_{\pi D^* D^*} \epsilon^{\delta\nu\theta\alpha} p_{2\theta} (p_2 - p_3)_\delta \frac{1}{u - m_{D^*}^2} \left(g_{\alpha\beta} - \frac{(p_2 - p_3)_\alpha (p_2 - p_3)_\beta}{m_{D^*}} \right) \times \\ g_{\psi D^* D^*} \left[(p_2 - p_3 - p_1)_\sigma g_{\mu\beta} + (p_1 + p_4)_\beta g_{\mu\sigma} - (p_2 - p_3 + p_4)_\mu g_{\sigma\beta} \right] \quad (19)$$

$$\mathcal{M}_{\mu\nu\sigma}^{3e} = -g_{\psi D^* D^* \pi} \epsilon^{\sigma\mu\theta\nu} p_{3\theta} + h_{\psi D^* D^* \pi} \epsilon^{\sigma\mu\theta\nu} p_{4\theta} \quad (20)$$

Finally the cross section for these processes is obtained with:

$$\frac{d\sigma}{dt} = \frac{1}{N} \frac{1}{64\pi \mathbf{p}_i^2} \sum_{spin} |\mathcal{M}^2| \quad (21)$$

where \mathbf{p}_i^2 a three-momentum squared in the center of mass system and the factor $\frac{1}{N}$ comes from the average over the initial state polarizations.

As extensively discussed in previous works, although the above lagrangians and amplitudes are quite satisfactory from the point of view of symmetry requirements, their straightforward application to the computation of cross sections leads to unacceptably large results. This comes from the fact that the exchanged particles may be far off-shell and therefore they enter (or leave) a vertex with a very different resolving power. In one extreme case considered in the recent past [26], a virtual J/ψ probing a D meson, had the behavior of a parton (!). Of course, when this happens, the compact J/ψ almost misses the large D and as a consequence the cross section of the whole process drops significantly. This physics of spatial extension and resolving power is contained in the form factors. It has been realized by many authors that calculations with and without form factors lead to results differing by up to two orders of magnitude! Therefore we simply *can not ignore the form factors*. We must include them in order to obtain reliable results!

Looking at the diagrams in Figures 1, 2 and 3 we notice that we need the following form factors (and the corresponding coupling constants):

$$g_{\pi DD^*}^{(D^*)}(t) \quad g_{\psi DD}^{(D)}(t) \quad g_{\psi DD^*}^{(D^*)}(t) \quad g_{\psi DD^*}^{(D)}(t) \quad g_{\psi D^* D^*}^{(D^*)}(t) \quad g_{\pi D^* D^*}^{(D^*)}(t) \quad (22)$$

where t is the usual momentum transfer squared and in the superscript in parenthesis we denote the off-shell particle. This is an important distinction, because the form factors in the same vertex are very different when different particles are off-shell. The most reliable way to compute these factors is with the use of the QCD sum rules techniques. The first one of the list was calculated in [27], the second in [26], the third and fourth in [28], the fifth in [25] and they read:

$$g_{\pi D^* D}^{(D)}(t) = 17.9 \left(\frac{(3.5 \text{ GeV})^2 - m_D^2}{(3.5 \text{ GeV})^2 - t} \right) = h_4(t, m_D^2) \quad (23)$$

$$g_{\psi D D}^{(D)}(t) = 5.8 \left(e^{-\left(\frac{20-t}{15.8}\right)^2} \right) = h_3(t) \quad (24)$$

$$g_{\psi D D^*}^{(D^*)}(t) = 20 \left(e^{-\left(\frac{27-t}{18.6}\right)^2} \right) = h_1(t) \quad (25)$$

$$g_{\psi D D^*}^{(D)}(t) = 13 \left(e^{-\left(\frac{26-t}{21.2}\right)^2} \right) = h_2(t) \quad (26)$$

$$g_{\pi D^* D^*}^{(\pi)}(t) = 4.8 \left(e^{\left(\frac{t}{6.8}\right)} \right) = h_6(t, m_\pi^2) \quad (27)$$

$$g_{\psi D^* D^*}^{(D^*)}(t) = 6.2 \left(e^{\left(\frac{t}{3.55}\right)} \right) = h_5(t) \quad (28)$$

The last form factor in (22) will be calculated below.

III. THE $\pi D^* D^*$ FORM FACTOR

In this section we shall, for the first time, compute the $\pi D^* D^*$ form factor using QCDSR [29,30]. In this approach, the short range perturbative QCD is extended by an OPE expansion of the correlators, which results in a series in powers of the squared momentum with Wilson coefficients. The convergence at low momentum is improved by using a Borel transform. The expansion involves universal quark and gluon condensates. The quark-based calculation of a given correlator is equated to the same correlator, calculated using hadronic degrees of freedom via a dispersion relation, providing sum rules from which a hadronic quantity can be estimated.

We shall use the three-point function to evaluate the $D^* D^* \pi$ form factor for an off-shell D^* meson, following the procedure suggested in ref. [31] and further extended in [28]. This means that we shall calculate the correlators for a D^* off-shell and then for a π off-shell, requiring that the corresponding extrapolations to the respective poles lead to the same unique coupling constant.

The three-point function associated with a $D^* D^* \pi$ vertex with an off-shell D^* meson is given by

$$\Gamma_{\mu\nu}^{(D^*)}(p, p') = \int d^4x d^4y \langle 0 | T \{ j_5(x) j_\nu(y) j_\mu^\dagger(0) \} | 0 \rangle e^{ip' \cdot x} e^{i(p-p') \cdot y}, \quad (29)$$

where $j_5 = i\bar{u}\gamma_5 d$, $j_\nu = \bar{c}\gamma_\nu u$ and $j_\mu = \bar{c}\gamma_\mu d$ are the interpolating fields for the π^- , D^{*0} , and D^{*-} respectively with u , d and c being the up, down, and charm quark fields.

The phenomenological side of the vertex function, $\Gamma_{\mu\nu}(p, p')$, is obtained by the consideration of π and D^* state contributions to the matrix element in Eq. (29):

$$\begin{aligned} \Gamma_{\mu\nu}^{(phen)}(p, p') &= \frac{m_\pi^2 m_{D^*}^2}{m_u + m_d} \frac{F_\pi f_{D^*}^2 g_{D^* D^* \pi}^{(D^*)}(q^2)}{(q^2 - m_{D^*}^2)(p^2 - m_{D^*}^2)(p'^2 - m_\pi^2)} \times \\ &\quad \varepsilon^{\mu\nu\lambda\delta} p_\lambda p'_\delta + \text{higher resonances}. \end{aligned} \quad (30)$$

To derive Eq. (30) we have made use of

$$\langle D^{*-}(p) | \pi^-(p') D^{*0}(q) \rangle = i g_{D^* D^* \pi}^{(D^*)}(q^2) \varepsilon^{\alpha\gamma\lambda\delta} p_\delta q_\lambda \epsilon_\alpha(p) \epsilon_\gamma^*(q) \quad (31)$$

where $q = p - p'$, and the decay constants F_π and f_{D^*} are defined by the matrix elements

$$\langle 0 | j_5 | \pi(p') \rangle = \frac{m_\pi^2 F_\pi}{m_u + m_d}, \quad (32)$$

and

$$\langle 0 | j_\mu | D^*(p) \rangle = m_{D^*} f_{D^*} \epsilon_\mu(p), \quad (33)$$

where ϵ^ν is the polarization of the vector meson. The contribution of higher resonances and continuum in Eq. (30) will be taken into account as usual in the standard form of ref. [34], through the continuum thresholds s_0 and u_0 , for the D^* and π mesons respectively.

The QCD side, or theoretical side, of the vertex function is evaluated by performing Wilson's operator product expansion (OPE) of the operator in Eq. (29). Writing $\Gamma_{\mu\nu}$ in terms of the invariant amplitude,

$$\Gamma_{\mu\nu}(p, p') = \Lambda(p^2, p'^2, q^2) \varepsilon^{\mu\nu\lambda\delta} p_\lambda p'_\delta, \quad (34)$$

we can write a double dispersion relation for the invariant amplitude, Λ , over the virtualities p^2 and p'^2 holding $Q^2 = -q^2$ fixed:

$$\Lambda^{(D^*)}(p^2, p'^2, Q^2) = -\frac{1}{4\pi^2} \int_{m_Q^2}^{s_0} ds \int_0^{u_0} du \frac{\rho(s, u, Q^2)}{(s - p^2)(u - p'^2)}, \quad (35)$$

where $\rho(s, u, Q^2)$ equals the double discontinuity of the amplitude $\Gamma(p^2, p'^2, Q^2)$ on the cuts $m_Q^2 \leq s \leq \infty$, $0 \leq u \leq \infty$, which can be evaluated using Cutkosky's rules. Finally, in order to suppress the condensates of higher dimension and at the same time reduce the influence of higher resonances we perform a standard Borel transform [29]:

$$\Pi(M^2) \equiv \lim_{n, Q^2 \rightarrow \infty} \frac{1}{n!} (Q^2)^{n+1} \left(-\frac{d}{dQ^2} \right)^n \Pi(Q^2) \quad (36)$$

($Q^2 = -q^2$ and the squared Borel mass scale $M^2 = Q^2/n$ is kept fixed) in both variables $P^2 = -p^2 \rightarrow M^2$ and $P'^2 = -p'^2 \rightarrow M'^2$ and equate the two representations described above. We get the following sum rule:

$$\begin{aligned} \frac{m_\pi^2 m_{D^*}^2}{m_u + m_d} F_\pi f_{D^*}^2 g_{\pi D^* D^*}^{(D^*)}(Q^2) e^{-m_\pi^2/M'^2} e^{-m_{D^*}^2/M^2} = (Q^2 + m_{D^*}^2) \left[\langle \bar{q}q \rangle \exp(-m_c^2/M^2) \right. \\ \left. - \frac{1}{4\pi^2} \int_{m_c^2}^{s_0} ds \int_0^{u_{max}} du \exp(-s/M^2) \exp(-u/M'^2) f(s, t, u) \theta(u_0 - u) \right] \end{aligned} \quad (37)$$

where $t = -Q^2$,

$$f(s, t, u) = \frac{3m_c u (2m_c^2 - s - t + u)}{[\lambda(s, u, t)]^{3/2}}, \quad (38)$$

$\lambda(s, u, t) = s^2 + u^2 + t^2 - 2su - 2st - 2tu$, and $u_{max} = s + t - m_c^2 - \frac{st}{m_c^2}$.

We use the standard values for the numerical parameters: $m_{D^*} = 2.01$ GeV, $m_\pi = 140$ MeV, $F_\pi = \sqrt{2} \times 93$ MeV, $f_{D^*} = 240$ MeV, $m_u + m_d = 14$ MeV, $m_c = 1.3$ GeV, $\langle \bar{q}q \rangle = -(0.23)^3$ GeV³. For the continuum thresholds we take $s_0 = (m_{D^*} + \Delta_s)^2$ with $\Delta_s = 0.5 \pm 0.1$ GeV and $u_0 = 1.4 \pm 0.2$ GeV².

In Fig. 4 we show the perturbative (dotted line) and the quark condensate (dashed line) contributions to the form factor $g_{\pi D^* D^*}^{(D^*)}(Q^2)$ at $Q^2 = 0.5$ GeV² as a function of the Borel mass M^2 at a fixed ratio $M'^2/M^2 = 0.64/(m_{D^*}^2 - m_c^2)$. We see that the quark condensate contribution is bigger than the perturbative contribution for values of the Borel mass smaller than ~ 4.5 GeV². However, the sum of the both contributions for the form factor, is a very stable result as a function of the Borel mass. The quark condensate contribution grows with Q^2 while the perturbative contribution decreases. This imposes a limitation over the region of Q^2 that we can use to study the Q^2 dependence of the form factor. Fixing $M^2 = 10$ GeV², in Fig. 5 we show, through the filled circles, the momentum dependence of $g_{\pi D^* D^*}^{(D^*)}(Q^2)$.

Since the present approach can not be used at $Q^2 < 0$, in order to extract the $g_{\pi D^* D^*}$ coupling from the form factor, we need to extrapolate the curve to the mass of the off-shell meson D^* . In order to do this we fit the QCDSR results with an analytical expression. We have obtained a good fit using an exponential form:

$$g_{\pi D^* D^*}^{(D^*)}(Q^2) = 4.8 e^{-Q^2/6.8} \text{ GeV}^{-1}, \quad (39)$$

where 6.8 is in units of GeV². This fit is also shown in Fig. 5 through the solid line. From Eq.(39) we get $g_{\pi D^* D^*} = g_{\pi D^* D^*}^{(D^*)}(Q^2 = -m_{D^*}^2) = 8.7 \text{ GeV}^{-1}$. To check the consistency of the calculation, we also evaluate the form factor at the same vertex, but for an off-shell pion. In this case we have to evaluate the three-point function

$$\Gamma_{\mu\nu}^{(\pi)}(p, p') = \int d^4x d^4y \langle 0 | T \{ j_\nu(x) j_5(y) j_\mu^\dagger(0) \} | 0 \rangle e^{ip' \cdot x} e^{i(p-p') \cdot y} . \quad (40)$$

Proceeding in a similar way we obtain the following sum rule:

$$\frac{m_\pi^2 m_{D^*}^2}{m_u + m_d} F_\pi f_{D^*}^2 g_{\pi D^* D^*}^{(\pi)}(Q^2) e^{-m_{D^*}^2/M'^2} e^{-m_{D^*}^2/M^2} = (Q^2 + m_\pi^2) \left[-\frac{1}{4\pi^2} \int_{s_{min}}^{s_0} ds \int_{u_{min}}^{u_0} du e^{-s/M^2} e^{-u/M'^2} \frac{3m_c t(s+u-t-2m_c^2)}{[\lambda(s, u, t)]^{3/2}} \right] \quad (41)$$

where $u_{min} = m_c^2 - \frac{m_c^2 t}{s - m_c^2}$ and $s_{min} = m_c^2(1 - \frac{t}{u_0 - m_c^2})$. Now we use $u_0 = (m_{D^*} + \Delta_u)^2$ with $\Delta_u = 0.5 \pm 0.1$ GeV, and $M^2 = M'^2$. The results are also rather stable as a function of the Borel mass. We also got a good fit of the QCDSR results for $g_{\pi D^* D^*}^{(\pi)}(Q^2)$ using an exponential form:

$$g_{\pi D^* D^*}^{(\pi)}(Q^2) = 8.5 e^{-Q^2/3.4} \text{ GeV}^{-1}, \quad (42)$$

where 3.4 is in units of GeV^2 . This fit is also shown in Fig. 5 through the dot-dashed line. From Eq.(42) we get $g_{\pi D^* D^*} = g_{\pi D^* D^*}^{(\pi)}(Q^2 = -m_\pi^2) = 8.5 \text{ GeV}^{-1}$.

Considering the uncertainties in the continuum thresholds, and the difference in the values of the coupling extracted when the D^* or π mesons are off-shell, our result for the $\pi D^* D^*$ coupling constant is

$$g_{\pi D^* D^*} = 8.6 \pm 1.0 \text{ GeV}^{-1}, \quad (43)$$

The triple vertex couplings were calculated as explained above. The quartic vertex couplings could not be obtained with QCDSR and we have used the prescription given in [17]:

$$g_{\psi D D \pi} = \left(\frac{\sqrt{3}}{6} - \frac{1}{4} \right) \frac{g_a N_c}{16 \pi^2 F_\pi^3} \quad (44)$$

$$g_{\psi D^* D \pi} = \frac{1}{2} g_{\psi D D} g_{D^* D \pi} \quad (45)$$

$$g_{\psi D^* D^* \pi} = \frac{1}{2} \frac{g_a^3 N_c}{32 \pi^2 F_\pi} \quad (46)$$

where g_a is obtained from:

$$g_{\psi D^* D} = \frac{\sqrt{2}}{4\sqrt{3}} \frac{g_a^2 N_c}{16 \pi^2 F_\pi} \quad (47)$$

In the above expressions $N_c = 3$ and the triple vertex couplings are taken from our calculations. For completeness we present in Table I all the couplings.

$g_{D^* D \pi}$	17.9
$g_{\psi D^* D}$	4.0 GeV^{-1}
$g_{\psi D D}$	5.8
$g_{\psi D^* D^*}$	6.2
$g_{D^* D^* \pi}$	8.6 GeV^{-1}
$g_{\psi D D \pi}$	10.0 GeV^{-3}
$g_{\psi D^* D \pi}$	51.9
$g_{\psi D^* D^* \pi}$	57.0 GeV^{-1}

TABLE I. Coupling constants used in the numerical calculations. The first four were calculated with QCDSR and the last three were obtained with the prescription of [17]

IV. THE CROSS SECTIONS

Having all the needed form factors, we now proceed to the evaluation of the cross sections. As in previous calculations, these cross sections for secondary J/ψ production will be related to the annihilation through detailed balance:

$$\sigma_{(3+4 \rightarrow 1+2)} = \sigma_{(1+2 \rightarrow 3+4)} \frac{(2S_1 + 1)(2S_2 + 1)}{(2S_3 + 1)(2S_4 + 1)} \frac{P_i^2}{P_f^2} \quad (48)$$

In figure 6 we show the J/ψ secondary production cross section as a function of \sqrt{s} , without form factors. In all figures, the channels $D\bar{D} \rightarrow J/\psi + \pi$, $D\bar{D}^* \rightarrow J/\psi + \pi$ and $D^*\bar{D}^* \rightarrow J/\psi + \pi$ are represented by solid, dashed and dotted lines respectively. In figure 7, with the help of (48) we show the corresponding inverse reactions. As it can be seen, the cross sections have the same order of magnitude in both directions. Figures 8 and 9 are the analogues of 6 and 7 when we include the form factors in the calculations. Of course, as we stressed in the introduction, only these last two figures correspond to realistic numbers. The comparison of the two sets of figures is interesting only to estimate the effect of form factors. In previous studies doing the same kind of comparison, as for example in [17], the introduction of form factors reduced the cross sections by factors ranging between 20 and 50 depending on the channel. In that work the form factor was the same for all vertices and the cut-off, not known, was estimated to be between 1 and 2 GeV. Our study is much more detailed and not only each vertex has its own form factor, but, depending on which particle is off-shell the form factor is different. The final effect of all these peculiarities is the reduction of the cross sections by a factor around 7. Although significant, this reduction is smaller than previously expected.

Figure 8 contains our main results. The plotted cross sections can be compared with the results of [22] and, more directly, with [5]. In figure 2 of [22], although the variables in the plot are different, we can observe the same trend and relative importance of the three channels. In that work, the results were obtained with the quark model of [15]. Our curves share some features with the results of [5], such as, for example, the dominance of the DD^* channel and the falling trend of the DD^* and D^*D^* channels. The behavior of the DD channel is quite different. In the energy range of $\sqrt{s} > 4.5$ GeV our cross sections are smaller by a factor of 2 (DD^*) or 5 (D^*D^* and DD). These discrepancies are large but they are expected since in [5] all channels include the final state $J/\psi + \rho$. We could not include it consistently because the form factors of the ρDD^* and ρD^*D^* vertices have not yet been studied with our techniques and are thus not available. In the model used by the Giessen group the cross sections for $D + \bar{D} \rightarrow J/\psi + \pi$ and $D + \bar{D} \rightarrow J/\psi + \rho$ are similar and the same conclusion holds for the other initial state open charm mesons. If this would remain true in the effective lagrangian approach, then our results including both final states would come closer to those of [5], giving thus a more theoretical support to the model considered there.

V. SUMMARY AND CONCLUSIONS

We have updated the calculations of the cross sections for J/ψ dissociation and production in the effective lagrangian approach. The novel feature introduced in this work is the use of the form factors (23) - (28) and especially (39), which was obtained here from QCDSR. We believe that our results are useful for numerical simulations of heavy ion collisions, such as those performed in [2–5] and also in [22–24]. The calculation of the cross sections of the processes considered here are complete. However, our program is not yet finished and there are still form factors to be calculated, such as ρDD^* and ρD^*D^* . These calculations are under way and we will eventually have all hadronic form factors.

Although no strong statement can be made without knowing the $D + \bar{D} \rightarrow J/\psi + \rho$ cross section, our results give partial support to the conclusion advanced in [5], namely that the open charm fusion cross sections are large enough to produce a sizeable number of “recreated” J/ψ ’s already in heavy ion collisions at RHIC.

Acknowledgements: This work has been supported by CNPq and FAPESP. We are deeply grateful to R. Azevedo for fruitful discussions and help with numerical codes.

[1] T. Matsui and H. Satz, Phys. Lett. **B178**, 416 (1986).

- [2] R. L. Thews, hep-ph/0206179; R. L. Thews and J. Rafelski, Nucl. Phys. **A698**, 575 (2002); R. L. Thews, M. Schroedter, J. Rafelski Phys. Rev. **C63**, 054905 (2001).
- [3] L. Grandchamp and R. Rapp, hep-ph/0209141; Nucl. Phys. **A709**, 415 (2002); Phys. Lett. **B523**, 60 (2001).
- [4] A. Polleri, T. Renk, R. Schneider and W. Weise, Phys. Rev. C **70**, 044906 (2004).
- [5] E.L. Bratkovskaya, W. Cassing and H. Stöcker, Phys. Rev. **C67**, 054905 (2003); W. Cassing, K. Gallmeister, E.L. Bratkovskaya, C. Greiner and H. Stöcker, Prog. Part. Nucl. Phys. **53**, 211 (2004).
- [6] E. Shuryak, J. Phys. **G30**, (2004) S1221.
- [7] B.Z. Kopeliovich, A. Polleri and J. Hüfner, Phys. Rev. Lett. **87**, 112302 (2001), and references therein.
- [8] F. O. Durães, F. S. Navarra and M. Nielsen, Phys. Rev. C **68**, (2003) 044904.
- [9] G. Bhanot and M.E. Peskin, Nucl. Phys. **B156** (1979) 391; M.E. Peskin, Nucl. Phys. **B156** (1979) 365;
- [10] D. Kharzeev and H. Satz, Phys. Lett. **B334** (1994) 155.
- [11] S.H.Lee and Y. Oh, J.Phys. **G28** (2002) 1903; Y. Oh, S. Kim, S. H. Lee, Phys. Rev. **C65** 067901 (2002).
- [12] F. Arleo, P.-B. Gossiaux, T. Gousset and J. Aichelin, Phys. Rev. **D65** (2002) 014005,
- [13] Taesoo Song and Su Houn Lee, hep-ph/0501252.
- [14] C.-Y. Wong, E. S. Swanson and T. Barnes, Phys. Rev. **C62** 045201 (2000), **C65** 014903 (2001).
- [15] K. Martins, D. Blaschke and E. Quack, Phys. Rev. **C51** (1995) 2723.
- [16] S.G. Matinyan and B. Müller, Phys. Rev. **C58** (1998) 2994.
- [17] Y. Oh, T. Song and S.H. Lee, Phys. Rev. **C63** (2001) 034901.
- [18] K.L. Haglin, Phys. Rev. **C61** (2000) 031902; K.L. Haglin and C. Gale, Phys. Rev. **C63** (2001) 065201.
- [19] Z. Lin and C.M. Ko, Phys. Rev. C62 (2000) 034903.
- [20] F.S. Navarra, M. Nielsen and M.R. Robilotta, Phys. Rev. **C64** (2001) 021901(R).
- [21] F. O. Durães, S. H. Lee, F. S. Navarra and M. Nielsen, Phys. Lett. B **564**, 97 (2003); F. O. Durães, H. c. Kim, S. H. Lee, F. S. Navarra and M. Nielsen, Phys. Rev. C **68**, 035208 (2003).
- [22] C.M. Ko, B. Zhang, X.N. Wang, X.F. Zhang, Phys. Lett. **B444**, 237 (1998).
- [23] P. Braun-Munzinger and K. Redlich, Eur. Phys. J. **C16**, 519 (2000).
- [24] B. Zhang, C. M. Ko, B. A. Li, Z. W. Lin and S. Pal, Phys. Rev. C **65**, (2002) 054909.
- [25] M. E. Bracco, M. Chiapparini, F. S. Navarra and M. Nielsen, Phys. Lett. **B605**, 326 (2005).
- [26] R.D. Matheus, F.S. Navarra, M. Nielsen and R. Rodrigues da Silva, Phys. Lett. **B541** 265 (2002).
- [27] F.S. Navarra, M. Nielsen, M.E. Bracco, M. Chiapparini and C.L. Schat, Phys. Lett. **B489**, 319 (2000); F.S. Navarra, M. Nielsen and M.E. Bracco, Phys. Rev. **D 65** (2002) 037502.
- [28] R.D. Matheus, F.S. Navarra, M. Nielsen and R. Rodrigues da Silva, hep-ph/0310280, to appear in Int. Journ. Mod. Phys. E.; R. Rodrigues da Silva, R. D. Matheus, F. S. Navarra and M. Nielsen, Braz. J. Phys. **34**, (2004) 236.
- [29] M.A. Shifman, A.I. and Vainshtein and V.I. Zakharov, Nucl. Phys. **B147**, 385 (1979).
- [30] L.J. Reinders, H. Rubinstein and S. Yazaki, Phys. Rep. **127**, 1 (1985).
- [31] M.E. Bracco, M. Chiapparini, A. Lozea, F.S. Navarra and M. Nielsen, Phys. Lett. **B 521** (2001) 1;
- [32] H. Kim and S.H. Lee, Eur. Phys. Jour. **C22** (2002) 707.
- [33] V.M. Belyaev, V.M. Braun, A. Khodjamirian and R. Ruckl, Phys. Rev. D **51** (1995) 6177.
- [34] B.L. Ioffe and A.V. Smilga, Nucl. Phys. **B232** 109 (1984).

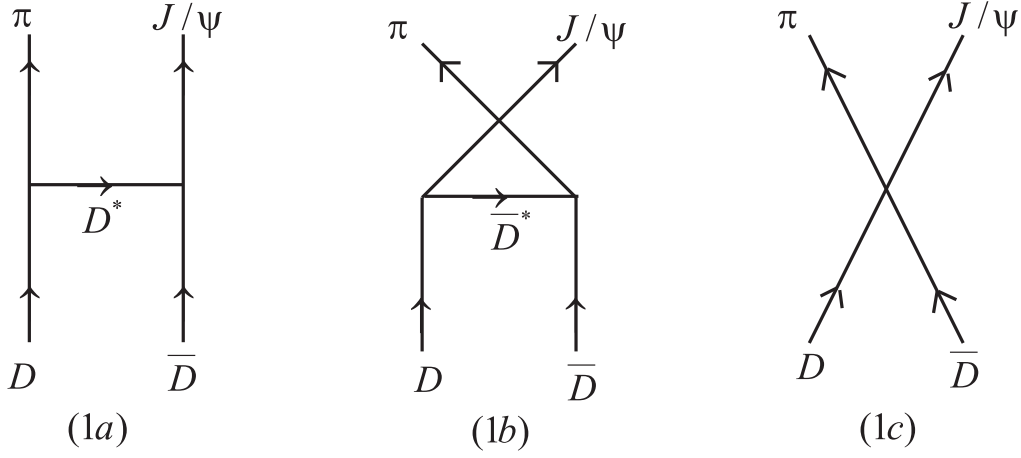


FIG. 1. Diagrams which contribute to the process $D\bar{D} \rightarrow J/\psi + \pi$

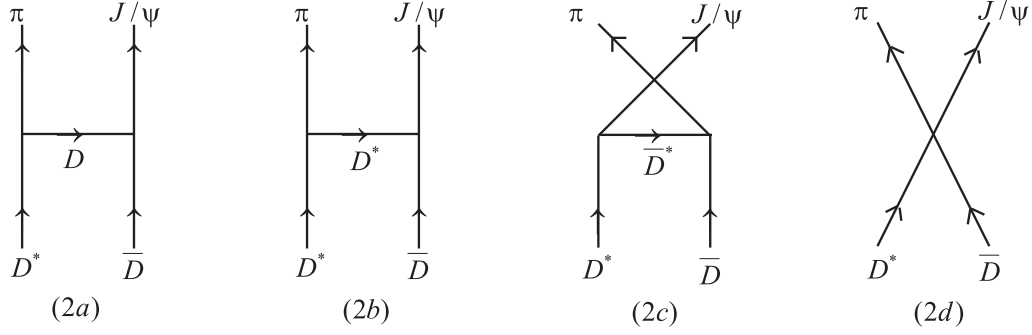


FIG. 2. Diagrams which contribute to the process $D^*\bar{D} \rightarrow J/\psi + \pi$

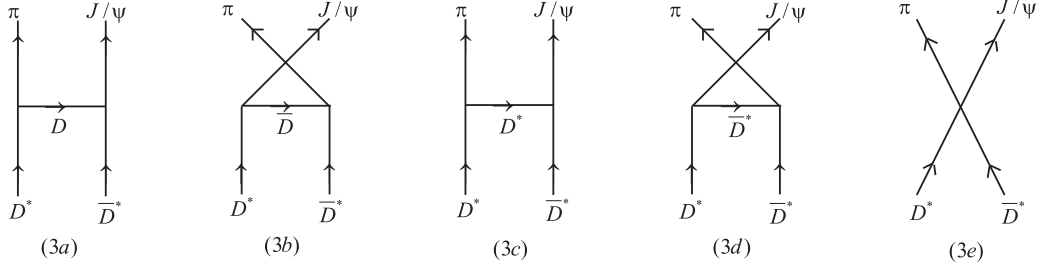


FIG. 3. Diagrams which contribute to the process $D^*\bar{D}^* \rightarrow J/\psi + \pi$

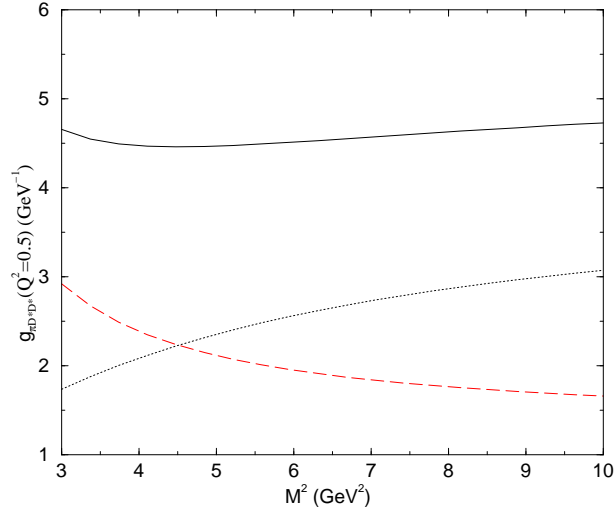


FIG. 4. M^2 dependence of the perturbative contribution (dotted line) and the quark condensate contribution (dashed line) to the $g_{\pi D^* D^*}^{(D^*)}(Q^2)$ at $Q^2 = 0.5 \text{ GeV}^2$. The solid line gives the final result for the form factor.

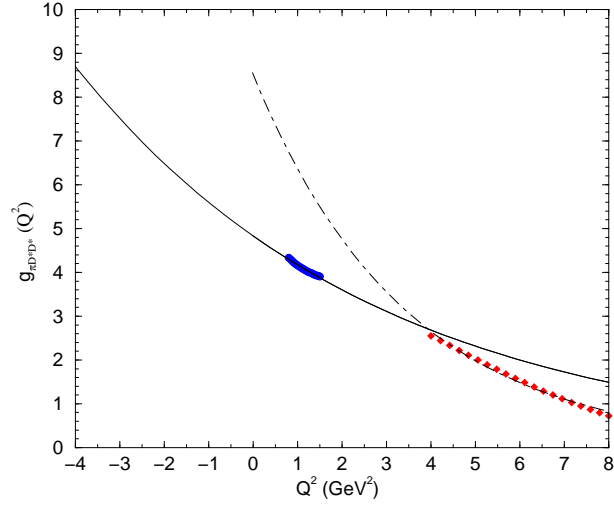


FIG. 5. Momentum dependence of the $\pi D^* D^*$ form factors. The solid and dot-dashed lines give the parametrization of the QCDSR results for $g_{\pi D^* D^*}^{(D^*)}(Q^2)$ (circles) and $g_{\pi D^* D^*}^{(\pi)}(Q^2)$ (squares) respectively.

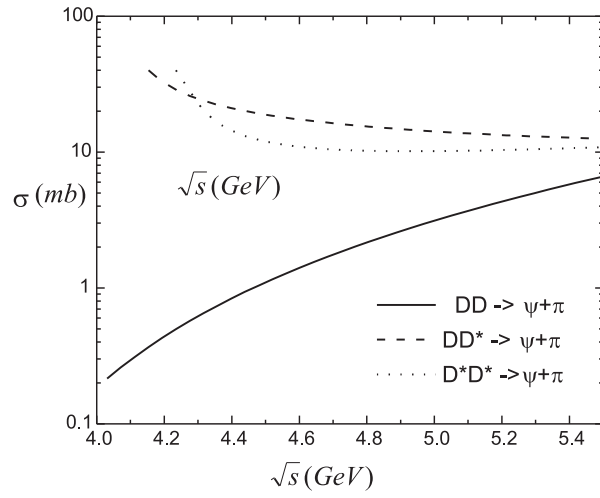


FIG. 6. J/ψ secondary production cross section without form factors

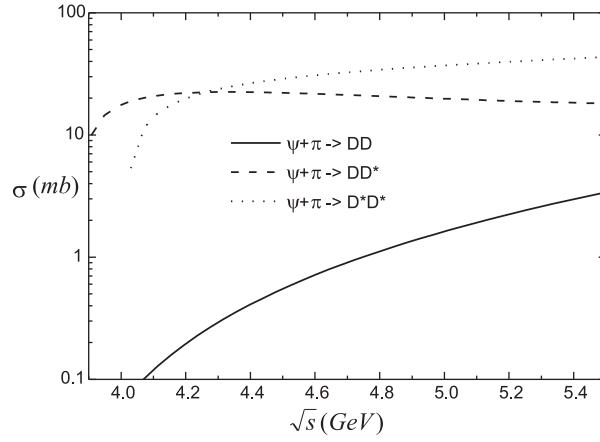


FIG. 7. J/ψ absorption cross section obtained through detailed balance without form factors

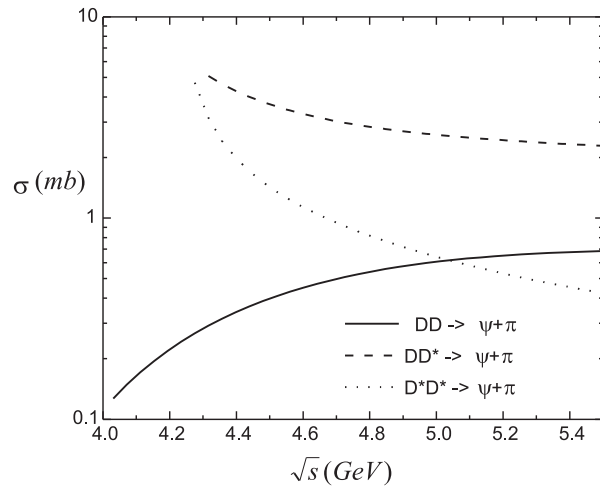


FIG. 8. J/ψ secondary production cross section with form factors

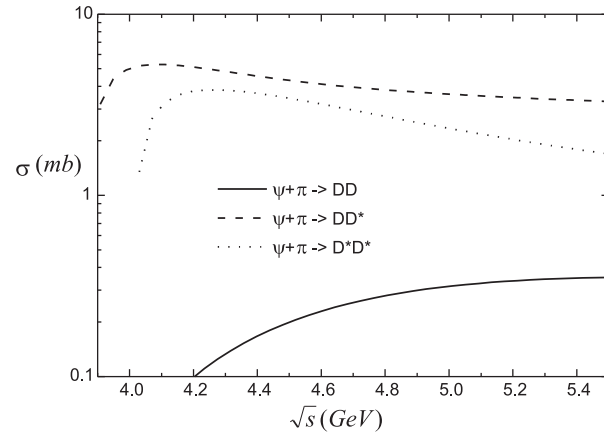


FIG. 9. J/ψ absorption cross section obtained through detailed balance with form factors